

The influence of osteoporotic bone structures of the pelvic-hip complex on stress distribution under impact load

KATARZYNA ARKUSZ^{1*}, TOMASZ KLEKIEL¹, TADEUSZ MARIAN NIEZGODA², ROMUALD BĘDZIŃSKI¹

¹ Department of Biomedical Engineering, Faculty of Mechanical Engineering, University of Zielona Góra, Zielona Góra, Poland.

² Department of Mechanics and Applied Computer Science,
Faculty of Mechanical Engineering, Military University of Technology, Warszawa, Poland.

Purpose: The aim of this study was to determine the effect of bone mineral density (BMD) on the stress distribution in pelvic-hip complex (PHC) model which included bone structures and soft tissues. Bone mass changes in osteoporosis and osteopenia were considered in this analysis. In addition, the relations between force direction and stress distribution causing PHC fractures were determined. *Methods:* This paper presents the development and validation of a detailed 3D finite element model with high anatomical fidelity of the PHC and BMD changes in trabecular and cortical bones, modelled based on CT scans. 10 kN loading was induced on a model consisting of 8 ligaments, the pelvis, sacrum, femur in front and side directions. *Results:* For validation, the results of this model were compared to physiological stress in standing position and previous results with high-energy crashes under side impact load. Analysis of side-impact indicated the influence of BMD on femoral neck fractures, acetabular cartilage and sacroiliac joint delaminations. Front-impact analysis revealed the inferior pubic ramus, femoral neck fractures and soft tissue injuries, i.e., acetabular cartilage and symphysis pubis in osteoporosis and osteopenia. *Conclusions:* The elaborated PHC model enables effective prediction of pelvis injuries in high-energy trauma, according to Young-Burgess classification, and the determination of the influence of BMD reduction on pelvis trauma depending on force direction. The correlation between BMD and stress distribution causing varying injuries was determined.

Key words: pelvic-hip complex (PHC), bone mineral density (BMD), finite element analysis (FEA), osteoporosis

1. Introduction

Osteoporosis is classified as one of the main civilization diseases and characterized by low bone mineral density and changes in compact bone microstructures. In 2010, the estimated prevalence of new diagnosed osteoporosis among American community was 8 mln women and 2 mln men, according to Burge et al. [4]. By 2020, the new osteoporotic diagnosis are projected to increase to 14 mln [21]. Osteoporotic changes in bone cause reduction in overall skeleton strength, which leads to excessive sensitivity to low-energy fractures, mainly located in hip bone (72%), vertebrae (6%) and pelvis (5%). More than 1.5 mln fractures per year is a result of osteoporosis, which

makes it a global, social and economical problem [4]. The most common injuries (60%) apply to fractures of the femoral neck and pelvis in patients aged 85 and over [4], [10], [13].

The occurrence and development of osteoporosis are associated with many factors, such as age, progressive bone demineralization or abnormal hormone levels [24]. A lack of estrogen in blood serum of postmenopausal women, which prevents the absorption and utilization of calcium, makes older woman most affected by osteoporosis. Due to the decrease in levels of estrogen, which is responsible for the management of the body calcium, more women, especially during and after menopause, suffer from osteoporosis [4], [8].

Osteoporotic changes are characterized by indirect and non-uniform decrease in bone density, particu-

* Corresponding author: Katarzyna Arkusz, Department of Biomedical Engineering, Faculty of Mechanical Engineering, University of Zielona Góra, ul. Licealna 9, 65-417 Zielona Góra, Poland. Phone: 604059548, E-mail: k.arkusz@ibem.uz.zgora.pl

Received: April 1st, 2017

Accepted for publication: November 28th, 2017

larly in trabecular bone. The annual rate of bone loss in women aged 38 and over has been calculated to be 0.3 percent per year, in postmenopausal women to be 1.2 percent, whereas in men to be 0.3–0.5 percent. This is due to the release of calcium and magnesium from bone, resulting in decreasing in trabecular bone thickness and bone volume loss [21]. The severity of osteoporosis depends on bone resorption activity and local biomechanical factors.

The development of osteoporosis significantly affects the decrease of the mechanical parameters of bone structures. According to Burr et al. [5], the decrease of collagen in bone tissue results in a strength loss up to 50%. Experimental studies employed on the sectional preparations pointed out that the average Young's modulus for normal bone tissue has value of 16.586 GPa (range 67–86 years), however for an osteoporotic bone it is much smaller, i.e., 11.554 GPa (range 67–91 years) [7]. According to Mazurkiewicz et al. [17] these value for people aged 53–76 is lower, and amounts to 15.7 GPa. Furthermore, tensile strength (from 117 MPa to 95.1 MPa) and yield strength (from 80.8 MPa to 75.8 MPa) tend to decrease with bone mineral density loss. Based on reports elaborated by the World Health Organization (WHO) and the National Osteoporosis Foundation (NOF), bone mineral density (BMD) higher than 833 mg/cm² for physiological bone, in the range 833–648 mg/cm² for osteopenia, and less than 648 mg/cm² for osteoporosis has a significant influence on bone mechanical properties [17]. Experimental research carried out by Rosholm et al. [20] confirmed the above classification and indicated the average BMD in age group 59–84 diagnosed with osteoporosis as 410 mg/cm². The lower elastic modulus (233.6 MPa), yield strength (5.3 MPa) and tensile strength (6.6 MPa) were measured for reduced BMD (380 mg/cm²) and located in cancellous bone of femoral head [27]. Demineralization process affects also the deterioration of elastic shear modulus (from 310 MPa to 247 MPa) and yield strength (from 3.3 MPa to 2.5 MPa) [14].

In view of the complicated geometric structure of pelvic-hip complex (PHC) and the problem to determine the elastic/visco-plastic material parameters of osteoporotic bone, previous numerical analyses were limited to modeling particular joint, i.e., lumbar vertebrae [15], [19], or hip [2], [9], [25]. The aim of the analysis carried out by Pitzen et al. [19] was to determine the critical forces causing disruption of bone structures in the lumbar spine. Numerical model was included in structure of the vertebral body consisting of cancellous and cortical structures, ligaments: anterior and posterior longitudinal, interspinous, yellow,

supraspinous and articular cartilages. More detailed model was elaborated by Liang et al. [15] and included a structure localized in T12-L1 spine, i.e., cortical and trabecular structures of vertebrae, the presence of the nucleus pulposus, the annulus fibrosus and various ligaments. Bauer et al. [2] characterized trabecular bone with varying radiological density (0, 70, 140 and 210 mg/cm³ by Hounsfield scale) by uniaxial compressive strength until axial force of 25–243 N, using the following material parameters: Young's modulus of 10 GPa, Poisson's ratio of 0.3. The analysis [9] carried out by Newton–Raphson method treated the femur as a homogeneous material with a Young's modulus equal to 10 GPa, Poisson's ratio of 0.4 and a density of 200 mg/cm².

Presented differences in biomechanical properties of bones characterized by abnormal BMD indicate varying stress/strain distribution under impact load, what may cause completely specific injuries than numerical analysis performed hitherto. Many numerical models of pelvic-hip complex have been elaborated and used to determine the stress distribution and the critical force in these structures under side impact load so far. According to Dawson et al. [6], the impact force which induced fracture of the pelvic bone was 8.6 kN (impact force – 129.2 N/s) on side impact. The region, which was the first to fracture was right pubic ramus, suggesting that frontal sections of pelvis are most susceptible to injury. The minimum force required to cause the left ischium and pubic ramus fractures was 10.28 kN at an impulse of 154.2 N/s (impact speed 44.6 km/h). Fractures of the left and right ischium, pubic ramus, left iliac fossa, and acetabulum are predicted under a peak force of 15.55 kN. Majumder et al. [16] indicated that the force causing the above-mentioned fractures was 16.98 kN. The superior pubic ramus has been damaged in the direction of the impact.

There are no models used in FEM analysis of osteoporotic changes in PHC in the literature. Characteristics carried out by Verhulp et al. [26] refer only to the stress distribution evaluation in the femur during a side falls. Forces in the range from 1 to 5 kN were applied to the pelvic-hip contact area and directed toward the center of the head. The elaborated model took into account the heterogeneity of bone – Young's modulus of the cortical and cancellous was 22.5 GPa and 15 GPa, respectively, bone mineral density was 0.917 and 0.976 g/cm² in the neck and trochanter of healthy bone and 0.496 and 0.656 g/cm² in the osteoporotic femurs, with Poisson's ratio of 0.3. The maximum stress occurred in the cortical bone in the femoral neck and the value of the critical force that caused its breaking was equal to 3.29 kN.

Up-to-date research indicates a significant role of osteoporotic changes in the mechanical properties of bone and its susceptibility to fracture. In addition, the significant prolongation of treatment time in patients with reduced mineral bone density was confirmed. It is, therefore, essential to know the mechanism of osteoporotic bone fracture and stress distribution in the osteoarticular system, not only in single bone analyzed until now, allowing the development of new crash protection features provide greater levels of injury protection. The aim of this study was to determine the effect of bone mineral density on the stress distribution in pelvic-hip complex which consisted of the bone and soft tissues. Changes in bone mineral density characteristic of osteoporosis and osteopenia were taken into account in this analysis. In addition, the relationship between direction of exerted force and stress characteristic result in bone fracture was investigated in some detail.

2. Materials and methods

2.1. The FE model of PHC

A detailed PHC model was elaborated using a computed tomography (CT) scans of a 25-year-old patient (woman, height: 1.64 m, weight: 52 kg) without osteoporotic changes in bones (T-score < -1), performed using an 8-row spiral CT with an accuracy of 2.5 mm. Bone structures were meshed with 8-node tetrahedral

finite elements (245262 elements), because tetrahedral element instead of cubic or hexahedral were adopted to represent a smooth surface which accurately depict stress in the concentration areas with the use of local grid densification.

Homogeneous orthotropic properties derived from the literature are assigned to the PHC model (Table 1). Herein we use the relationship between Young's modulus and bone mineral density for each bone according to Eqs. (1)–(4), where E_{cort} – Young's modulus of cortical bone, $E_{\text{FEMURtrab}}$ – Young's modulus of trabecular femur bone, $E_{\text{SACRUMtrab}}$ – Young's modulus of trabecular sacrum bone, $E_{\text{PELVIStrab}}$ – Young's modulus of trabecular pelvic bone, ρ – bone density [11]:

$$E_{\text{cort}} = 3.981\rho^{2.39} \quad (1)$$

$$E_{\text{FEMURtrab}} = 1.310\rho^{1.4} \quad (2)$$

$$E_{\text{SACRUMtrab}} = 1.540\rho - 0.058 \quad (3)$$

$$E_{\text{PELVIStrab}} = 2.0173\rho^{2.46} \quad (4)$$

The shear modulus of cortical and trabecular bones used in this analysis were calculated according to the Eq. (5), where G – shear modulus, E – Young's modulus and ν – Poisson's ratio as listed in Table 1.

$$G = \frac{E}{2(1 + \nu)} \quad (5)$$

Due to the lack of experimental data, pelvic ligaments were modeled as one-dimensional line elements, which act as linear springs where mechanical

Table 1. Elastic constants of cortical and trabecular bone of pelvic-hip complex modeled as orthotropic material for healthy bone, bone with osteopenia and osteoporosis, where cort – cortical bone, trab – trabecular [11]

| | Normal | | Osteopenia | | | Osteoporosis | | | | |
|------------------------------------|--------|------|------------|------|------|--------------|------|------|------|------|
| | Cort | Trab | Cort | Trab | | | Cort | Trab | | |
| | | | | F | S | P | | F | S | P |
| Density [g/cm^3] | 2.0 | 1.4 | 1.7 | 1.1 | | | 1.5 | 0.9 | | |
| Modulus of Elasticity [MPa] | | | | | | | | | | |
| E_1 | 6983 | 2029 | 4136 | 239 | 150 | 875 | 3066 | 201 | 132 | 643 |
| E_2 | 6983 | 2029 | 4136 | 239 | 150 | 875 | 3066 | 201 | 132 | 643 |
| E_3 | 18155 | 3195 | 10752 | 259 | 180 | 712 | 7972 | 239 | 170 | 619 |
| Poisson's Ratio | | | | | | | | | | |
| ν_{12} | 0.4 | 0.4 | 0.4 | 0.4 | 0.4 | 0.4 | 0.4 | 0.4 | 0.4 | 0.4 |
| ν_{23} | 0.25 | 0.25 | 0.25 | 0.25 | 0.25 | 0.25 | 0.25 | 0.25 | 0.25 | 0.25 |
| ν_{31} | 0.25 | 0.25 | 0.25 | 0.25 | 0.25 | 0.25 | 0.25 | 0.25 | 0.25 | 0.25 |
| Shear Modulus [MPa] | | | | | | | | | | |
| G_{12} | 4888 | 1420 | 2895 | 167 | 105 | 613 | 2146 | 141 | 92 | 450 |
| G_{23} | 4364 | 1268 | 2585 | 149 | 94 | 547 | 1916 | 126 | 83 | 402 |
| G_{31} | 11347 | 1997 | 6720 | 162 | 113 | 445 | 4983 | 149 | 106 | 387 |

Table 2. Material properties of ligaments responsible for stabilizing the pelvic-hip complex

| Ligament Name | Width | Length | Mean | | Stiffness | Young's modulus | Area | Thickness |
|---|-------|--------|-------|--------|-----------|-----------------|--------------------|-----------|
| | | | Width | Length | | | | |
| | s | L | s' | L' | k | E | A | g |
| | [mm] | [mm] | [mm] | [mm] | [N/m] | [MPa] | [mm ²] | [mm] |
| Lig. Sacroiliaca anteriora s. ventralia | | | | | | | | |
| 1 | 7.4 | 30 | 10 | 26.75 | 21000 | 355 | 1.58 | 0.1582 |
| 2 | 10.78 | 31 | | | | | | |
| 3 | 11.59 | 26 | | | | | | |
| 4 | 10.23 | 20 | | | | | | |
| Lig. Sacroiliaca posteriori s. dorsalna | | | | | | | | |
| 1 | 8.84 | 28 | 9.03 | 32.33 | 18900 | 355 | 1.72 | 0.1906 |
| 2 | 9.38 | 35 | | | | | | |
| 3 | 8.88 | 34 | | | | | | |
| Lig. Sacrotuberale | 5.95 | 36 | 5.95 | 36 | 12600 | 355 | 1.28 | 0.2147 |
| Lig. Sacrospinale | 10.74 | 106 | 10.74 | 106 | 22500 | 355 | 6.72 | 0.6255 |
| Poisson's Ratio | | | | | | | | |
| Cartilage sacrum-pelvis | | | | | | 54 | 0.2 | |
| Symphysis Cubica | | | | | | 54 | 0.2 | |

properties are shown in Table 2 [3]. The elaborated PHC model consists of the ligaments responsible for keeping the weight of the trunk and upper limbs, providing stability and attenuate forces on the lower extremities and the spine: anterior and posterior sacroiliac ligaments. Additional ligaments responsible for preventing the apex of sacrum from tilting farther back: sacrotuberous and sacrospinous ligaments.

The hip capsules on the left and right sides were modelled as the part of the acetabulum and provided connection of the hip and femur bones. The material properties for these capsules were estimated based on the tangent modulus determined by Hewitt et al. [12].

The Young modulus was calculated as the average stress measured from 0 to 80% of strain in the capsule. In the result, the mean value was assumed to be the same as for articular cartilage material in the acetabulum.

2.2. Loading and boundary conditions

The elaborated PHC model (Fig. 1) maps the sitting position of a driver/passenger resulting from ischial tuberosities support (Fig. 1A and B). Addition-

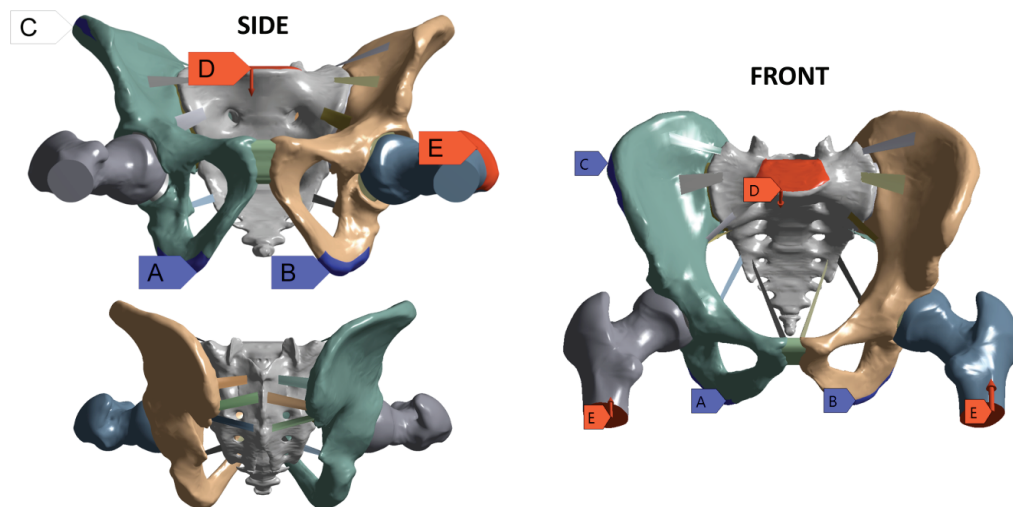


Fig. 1. The PHC model and boundary conditions of performed analysis: A, B – ischial tuberosities support, C – iliac crest support, D – physiological load of human body, E – impact load

ally, the iliac crest support was applied where the seatbelts are fastened (Fig. 1C). The model also takes into account the physiological load value 500 N acting perpendicularly to the base of sacrum and imitating the human body mass (Fig. 1D).

To constrain rigid body motion, the model translation was fixed in the horizontal direction (at the top of the sacrum bone by load of 500 N and at the bottom of the ischial tuberosities by fixed support) and in the vertical direction (at the iliac crest surface, by fixed support). Thus, no degrees of freedom remained. This assumption could be applied due to the analysis of principal stretches not taking into account the displacement of anatomical structures.

We also analyzed the stress distribution under impact load as a force value 10 kN – force causing first fracture in pelvic complex [6], [16], [26] loading in two directions (Fig. 1E):

- SIDE IMPACT – load acting perpendicularly to the greater trochanter of the femur
- FRONT IMPACT – load acting perpendicularly to the cross-section of femur

The above analysis was carried out using ANSYS 15.2. software.

3. Results

3.1. The PHC model validation

Validation of the elaborated PHC model (Fig. 1) was achieved through the simulation of physiological

stress distribution during sitting. To this end, the ischial tuberosities were supported and the load was imposed vertically onto the sacral promontory. The stress distribution under an axial compressive load of 500 N is shown in Fig. 2.

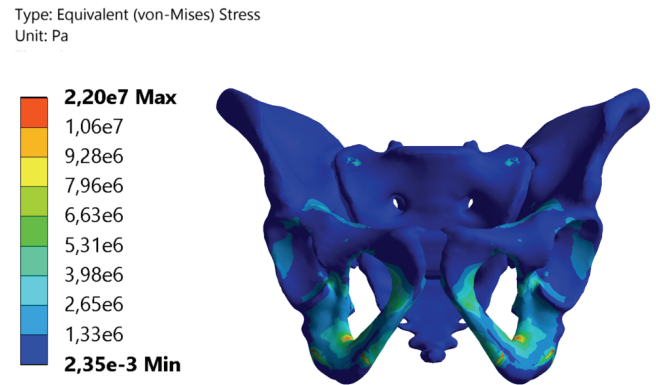


Fig. 2. Physiological stress distribution in pelvic complex under load of 500 N imposed onto the sacral promontory during sitting

The stress concentrated mainly on the surface of sacroiliac joint, lunate surface of the acetabulum, in particular on rami inferior ossis pubis, where the maximum stress value 22 MPa was localized.

The PHC model was also validated by the stress distribution under side and front impact load of 15 kN concentrated in greater trochanter and on cross-section of femur, respectively. The simulation results from the PHC model are shown in Fig. 3, with the maximum stress and fracture (stress > 135 MPa) occurring in ramus of ischium under forces acting in both directions. Other fractures are localized in pubic

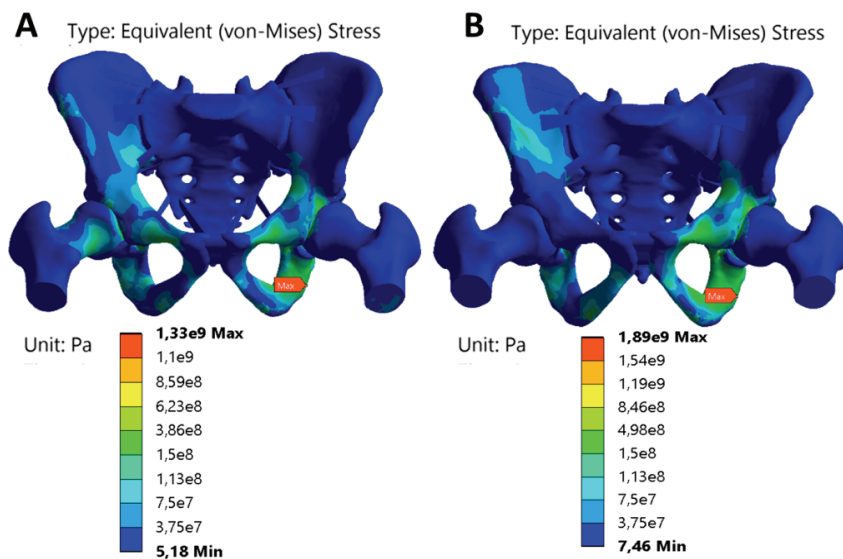


Fig. 3. Stress distribution of pelvic-hip complex under front (A) and side (B) impact load of 15 kN acting on the cross-section of femur and on the greater trochanter, respectively

rami. In the front impact case, the fractures of femur neck were additionally observed.

3.2. FE model boundary condition analysis

The stress distribution on the pelvis under side and front impact load (10 kN) was performed using the elaborated and validated PHC model in which bones

varies by bone mineral density. Obtained results are shown in the following charts: pelvic bone (Fig. 4), femur (Fig. 5), and sacrum (Fig. 6).

The analysis of the stress distribution in the pelvic bone (Fig. 4) showed the highest stress concentration in the body of the ischium and its fractures in each analyzed case under side and front impact load. The fracture of the body of the pubis was recorded only in bone with osteopenic and osteoporotic changes under front impact load. Stresses exceeding ultimate stress at failure (135 MPa) were observed in the bodies of the

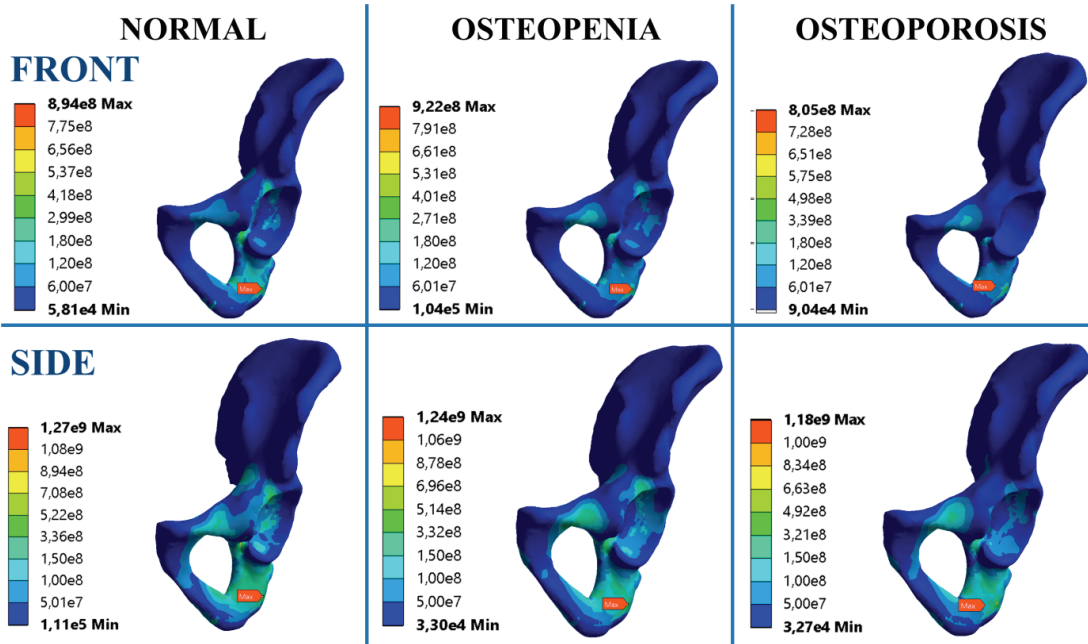


Fig. 4. Stress distribution in pelvic bone with varying bone mineral density under front and side impact having value of 10 kN

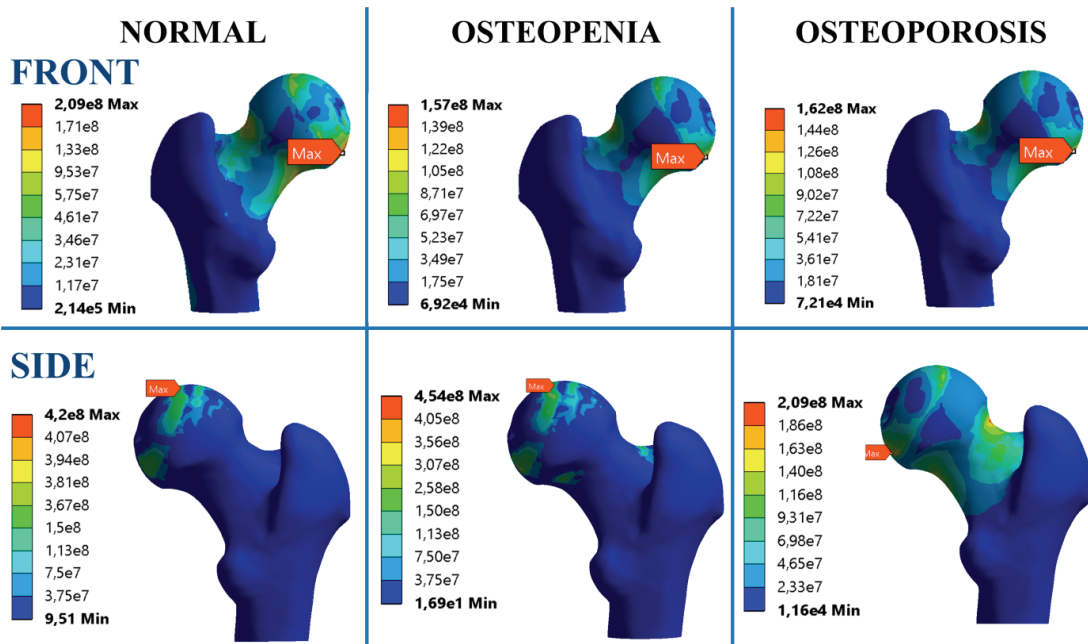


Fig. 5. Stress distribution in femur with varying bone mineral density under front and side impact having value of 10 kN

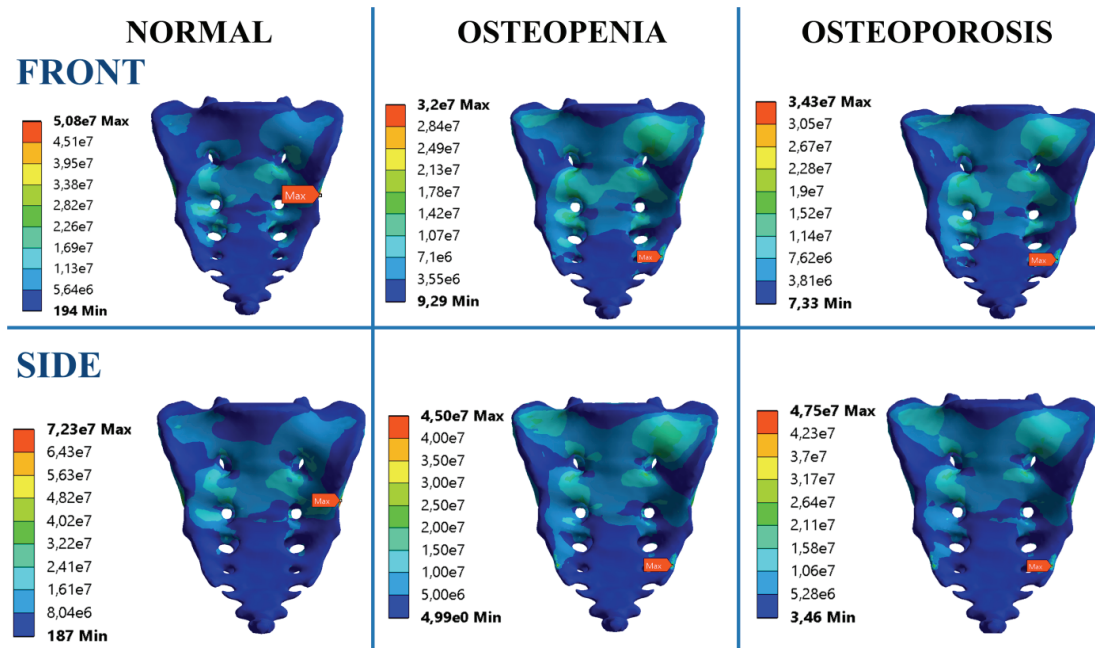


Fig. 6. Stress distribution in sacrum with varying bone mineral density under front and side impact having value of 10 kN

Table 3. Maximum stresses concentrate in soft tissue of the PHC model under side and front impact load with value of 10 kN

| Max. Equivalent Stress (von-Misses) [MPa] | | | |
|---|------------|------------|--------------|
| | Normal | Osteopenia | Osteoporosis |
| Side impact | | | |
| Symphysis Pubis | 21 | 50 | 50 |
| Left Articular Capsule of Hip | 406 | 418 | 218 |
| Right Articular Capsule of Hip | 4.5 | 15 | 12 |
| Left Sacroiliac Joint | 68 | 32 | 29 |
| Right Sacroiliac Joint | 55 | 25 | 25 |
| Front impact | | | |
| Symphysis Pubis | 16 | 31 | 34 |
| Left Articular Capsule of Hip | 311 | 326 | 174 |
| Right Articular Capsule of Hip | 163 | 183 | 184 |
| Left Sacroiliac Joint | 47 | 24 | 24 |
| Right Sacroiliac Joint | 52 | 22 | 22 |

ischium and pubis on side impact load, regardless of bone mineral density. Maximum stresses concentrated in the lower part of the head of the femur (Fig. 5) and the neck of the femur in the case of front impact load. Stresses exceeding the ultimate strength of bone were calculated for osteoporotic bone under two directions forces (max. stresses: 162 MPa). Forces of value 10 kN acting on the greater trochanter in side impact and cross-section of femur in front impact do not lead to fracture of sacrum bone, regardless of its BMD (Fig. 6).

The numerical PHC model has been widely applied to analyze the behavior of cartilages under compressive stress (Table 3). We have also reported an

acetabular labrum fracture during side impact and sacroiliac joint destruction under front impact.

4. Discussion

Osteoporosis is classified as one of the diseases of civilization, also called the “epidemic of the 21st century”, being not only a health problem, but also a socio-economic problem of today’s world. Apart from the development of pharmacological treatment of osteoporosis taken to prevent or slow down the bone degradation, it is also important to understand the

mechanism of osteoporotic bone fractures, to reduce or eliminate risk factors. Research and past numerical analyses have been related to the influence of bone mineral density on mechanical properties, development of computer system to aid diagnosis of osteoporosis or traumatological analysis of low-energy trauma (i.e., falls). The authors attempted to elaborate a numerical model of pelvic-hip complex with regard to bone mineral density and analyze the mechanism of osteoporotic fractures under impact load acting in different directions.

The failure criterion adopted for the numerical analysis in the present work is the ultimate stress for cortical bone: 135 MPa and for cartilage: 40 MPa [18].

Using the PHC model (Fig. 1), the predicted stress distribution in pelvic girdle during sitting (Fig. 2) is in accordance with analogical analysis performed in literature [28]. Zhou et al. [28] indicated the maximum stress concentration in greater sciatic notch. Stresses occur also in sacroiliac joint and acetabulum regions including ischium bones. Stress concentration regions are almost identical with our results. The difference in maximal stress obtained using the PHC model, i.e., 22 MPa, compared to 1.1 MPa described in literature [23], arises from varying mechanical parameters of two types of bone tissue used in our model. The influence of one- and two-phase biomechanical models of bone tissue were analyzed [17], [14], [26] and proved the two-phase model much more accurate [11]. The application of trabecular bone with reduced strength parameters (Table 1), compared to the cortical one, have an influence on higher stresses concentrated in bones. In addition, the FE model elaborated by Zhou et al. [28] contained the fifth lumbar vertebra and did not include the ligaments which cause stress distribution to the lower part of the pelvis-hip complex.

The second stage of validation was carried out for high-energy accidents using forces of 15 kN. According to research [6], [16], forces acting in two directions – side and front cause total destruction of pelvis and allow to compare these fractures with Tile, Young and Burgess classification [1]. Material properties of bone and soft tissue were used for normal BMD (T-score -1). According to boundary condition of the performed analysis, side impact acting at greater trochanter results in fractures of inferior ischium ramus and superior pubic ramus (Fig. 3A). Dawson et al. [6], whose pelvis model was validated by experimental measurement, obtained identical results indicating that the right superior pubic ramus fracture first occurred under side impact. Right inferior ischium ramus and right superior pubic ramus fractured under peak force of 15.55 kN and impulse of 233.3 N/s (at an impact speed of 50.5 km/h). The results of research

conducted by Majumder et al. [16] indicated that the first fracture of left superior ossis pubis on impact side under the force of 15.98 kN prove the elaborated PHC model correct. Validation of the PHC model in regard to front impact value of 15 kN (Fig. 3B) shows fractures of ischium and pubic rami, then the neck of the femur on the load side. The obtained results are in accordance with Young and Burgess classification [1].

Performed two-staged validation process proved to be correct for the elaborated PHC model, the chosen material properties and ensures that there are no hidden disconnections between the model and the physical testing. The previous analyses were performed within a single bone structure, without taking into account the soft tissue and the articular joint [2], [9], [15], [19], [25]. On the other hand, estimation of pelvis injuries using finite element method was performed only for bone without bone mineral changes [6], [16], [26]. Fractures of the ischium and head of the femur fractures were observed under side and front impact of 10 kN in model of pelvic girdle bone with normal BMD (T-score < -1). The changes in stress distribution of pelvis with force directions were demonstrated. Side impact loads cause stress concentration in the ischium and pubis bones (Fig. 4), in the neck and head of the femur (Fig. 5) and in the base of sacrum (Fig. 6), however, under front impact stress concentration was localized in superior ischial ramus (Fig. 4), the head of the femur (Fig. 5) and sacral foramina (Fig. 6). These stress distributions are also in accordance with Young and Burgess classification [1]. Performed numerical research [6], [16] also indicate the stress concentration in the above-mentioned regions under impact load.

Inclusion of bone mineral density and mechanical properties characteristic of osteopenia (Table 1) influence the destruction of pelvic-hip complex. The bone density set at 740.5 mg/cm² in the PHC model corresponds to T-score of -1.75 , an half of BMD range for osteopenia (T-score $-1 \div -2.5$). Tensile stress values and stress distribution are similar to the one studied for bone within the normal range of BMD. That is, only the advanced states of osteopenia affect the formation and extent of fractures. Significant changes are observed in the FE analysis of model consisting of osteoporotic bone (i.e., T-score > -2.5). The stress distribution in PHC under side impact load is changed with BMD loss. Impact load acting on the greater trochanter caused the head of the femur to fracture (Fig. 5) and total degradation of the left acetabulum (Table 3). This results in lower stress in the pelvic bone, concentrating in the ischium (Fig. 4) and its further transfer to the sacrum bone, mainly via the sac-

roiliac joints which are destroyed (Table 3). Bone density loss also causes the fracture of the femur and left acetabulum. Overwhelming loss of cancellous bone density (15–45%), compared to cortical (5–15%), in osteoporosis results in higher stress concentration in the frontal part of the pelvic girdle, resulting in symphysis pubis fracture (stress: 50 MPa, Table 3). The sacroiliac joints remain intact and the higher stress is localized in the sacrum bone (Fig. 6). The mechanism of pelvic-hip injuries under frontal impact load consists firstly of femur (Fig. 5) and acetabula (Table 3) fractures, then ischium and pubis bone (Fig. 4), and finally in sacroiliac joint injuries (Table 3). Loss of BMD results in greater stress in the midline directly over the symphysis pubis (from 16 to 31–34 MPa), similar to the side impact load. Interruption in the continuity of the pelvic ring was observed under front impact load.

The mechanism of stress distribution in pelvic complex depends on force direction and soft tissue biomechanics (Table 3). The large stress for the articular capsule presented in Table 3 suggests large displacements in the hip joint causing the hip capsule to extend over the ultimate strength designated by the Steward et al. [22]. These deformations can generate injuries such as sprains or tears of the hip joint capsule and the surrounding ligaments. In the case of front impact load the main role in stress distribution is played by acetabula and articular cartilages and it lost its function in each analyzed cases. This results in higher stress concentration in cortical femur bone and fractures occurred in pelvic bone, which is compounded by osteoarthrotic changes in cartilage result in greater and more-rapid deformation of the tissue than normal. The extent of the pelvic fracture under side impact load is related with simultaneous action of articular cartilage, symphysis pubic and side sacroiliac joint.

Numerical analysis performed with the use of the PHC model indicates the femur as a part most vulnerable to fracture. These results are consistent with statistical analysis of pelvic fracture [4] and experimental studies on microarchitectural changes in the femur [10], [13]. It has been shown that the femur bones are particularly vulnerable to the degenerative changes and loss of rod-like trabecular structure, which causes an increase in stress transmitted to the adjacent bone and the destruction of cartilages [10].

5. Conclusions

The stress distribution in pelvic-hip complex in diseases such as osteopenia and osteoporosis is investi-

gated under impact loading condition. A bone mineral density changes model is used in the FE simulation of the PHC to examine the extent and sequence of pelvic fracture and soft tissue influence on stress transmission under varying force directions. The elaborated PHC model with varying BMD in each bone and multiple ligaments and cartilages described as inhomogeneous ortho-tropic material. The detailed PHC model was validated by comparison to the model described in literature, experimentally validated back during physiological standing and under side impact load.

Executed numerical analysis showed significant effect of bone mineral density on stress distribution in the PH complex under impact load. It was also demonstrated that the force directions affect the stress distribution and not independently of BMD concentration in the same regions. The maximum stress concentration in the femur (in the neck of the femur for side impact and in the head and neck of the femur for front impact) and its transfer through the joint causing pelvic bone, cartilages and symphysis pubic were confirmed.

The mechanism of damage evolution coupled with yielded criterion is considered as one of the unclear subjects in failure analysis of cortical bone materials and still debatable. The elaborated complex model can be useful in further simulation of PHC fractures depending on interaction between drugs and fracture, hormone influence on bone strength and implant loosening mechanism in osteoporotic patients.

Acknowledgments

This investigation was supported by a research grant, as a part of the project DOBR-BIO/22/13149/2013: “*Improvement of safety and protection of soldiers on missions through military-medical and technical operations*” sponsored by the National Centre for Research and Development in Poland.

References

- [1] ALTON T.B., GEE A.O., *Classifications in Brief: Young and Burgess Classification of Pelvic Ring Injuries*, Clin. Orthop. Relat. Res., 2014, 472, 2338–2342.
- [2] BAUER J.S., SIDORENKO I., MUELLER D., BAUM T., ISSEVER A.S., ECKSTEIN F., RUMMENY J., LINK T.M., RAETH Ch.W., *Prediction of bone strength by μ CT and MDCT-based finite-element models: How much spatial resolution is needed?*, Eur. J. Radiol., 2014, 83, 36–42.
- [3] BĘDZIŃSKI R., WYSOCKI M., KOBUS K., SZOTEK S., KOBIELARZ M., KUROPKA P., *Biomechanical effect of rapid mucoperiosteal palatal tissue expansion with the use of osmotic expanders*, J. Biomech., 2011, 44, 1313–1320.

- [4] BURGE R., DAWSON-HUGHES B., SOLOMON D.H., WONG J.B., KING A., TOSTESON A., *Incidence and Economic Burden of Osteoporosis-Related Fractures in the United States 2005–2025*, J. Bone Min. Res., 2006, 3, 467–475.
- [5] BURR D.B., *The contribution of the organic matrix to bone's material properties*, Bone, 2002, 31, 8–11.
- [6] DAWSON J.M., KHMELNIKER B.V., MCANDREW M.P., *Analysis of the structural behavior of the pelvis during lateral impact using the finite element method*, Accid. Anal. Prev., 1999, 31, 109–119.
- [7] DICKENSON R.P., HUTTON W.C., STOTT J.R.R., *The mechanical properties of bone in osteoporosis*, J. Bone Joint Surg., 1981, 63, 233–238.
- [8] DY CH.J., LAMONT L.E., TON Q.V., LANE J.M., *Sex and Gender Considerations in Male Patients With Osteoporosis*, Clin. Orthop. Relat. Res., 2011, 469, 1906–1912.
- [9] FILIPIAK J., KRAWCZYK A., MORASIEWICZ L., *Distribution of radiological density in bone regenerate in relation to cyclic displacements of bone fragments*, Acta Bioeng. Biomech., 2009, 11, 3, 3–9.
- [10] HEINI P.F., FRANZ T., FANKHAUSER CH., GASSER B., GANZ R., *Femoroplasty-augmentation of mechanical properties in the osteoporotic proximal a biomechanical investigation of PMMA reinforcement in cadaver bones*, Clin. Biomech., 2004, 19, 506–512.
- [11] HELGASON B., PERILLI E., SCHILEO E., TADDEI F. BRYNJOLFSSON S., VICECONTI M., *Mathematical relationships between bone density and mechanical properties: a literature review*, Clin. Biomech., 2008, 23, 135–46.
- [12] HEWITT J., GUILAK F., GLISSON R., VAIL P., *Regional material properties of the human hip joint capsule ligaments*, J. Orthop. Res., 2001, 19, 359–364.
- [13] HUYBRECHTS K.F., ISHAK K.J., CARO J.J., *Assessment of compliance with osteoporosis treatment and its consequences in a managed care population*, Bone, 2006, 38, 922–928.
- [14] LI B., ASPDEN R.M., *Composition and Mechanical Properties of Cancellous Bone from the Femoral Head of Patients with Osteoporosis or Osteoarthritis*, J. Bone Min. Res., 1997, 12, 641–651.
- [15] LIANG D., YE L., JIANG X.B., YANG P., ZHOU G.Q., YAO Z.S., ZHANG S.C., YANG Z.D., *Biomechanical effects of cement distribution in the fractured area on osteoporotic vertebral compression fractures: a three-dimensional finite element analysis*, J. Surg. Res., 2015, 195, 246–256.
- [16] MAJUMDER S., ROYCHOWDHURY A., PAL S., *Three-dimensional finite element simulation of pelvic fracture during side impact with pelvis-femur-soft tissue complex*, Int. J. Crashworthines, 2008, 13, 313–329.
- [17] MAZURKIEWICZ A., TOPOLIŃSKI T., *Relation between structure, density and strength of the human trabecular bone*, Acta Bioeng. Biomech., 2009, 11, 55–61.
- [18] PAL S., *Design of Artificial Human Joints and Organs*, Springer, Hardcover, ISBN: 978-1-4614-6254-5, 2014.
- [19] PITZEN T., GEISLET F., MATTHIS D., MULLER-STORZ H., BARBIER D., STEUDEL W.I., FELDGES A., *A finite element model for predicting the biomechanical behavior of the human lumbar spine*, Control Eng. Pract., 2002, 10, 83–90.
- [20] ROSHOLM A., HYLDSTRUP L., BAKSGAARD L., GRUNKIN M., THODBERG H.H., *Estimation of Bone Mineral Density by Digital X-ray Radiogrammetry: Theoretical Background and Clinical Testing*, Osteoporosis Int., 2001, 12, 961–969.
- [21] SEHMISCH S., GALAL R., KOLIOS L., TEZYAL M., DULLIN C., ZIMMER S., STUERMER K.M., STUERMER E.K., *Effects of low-magnitude, high-frequency mechanical stimulation in the rat osteopenia model*, Osteoporos. Int., 2009, 20, 1999–2008.
- [22] STEWART K.J., EDMONDS-WILSON R.H., BRAND R.A., BROWN T.D., *Spatial distribution of hip capsule structural and material properties*, J. Biomech., 2002, 35, 1491–1498.
- [23] STROM O., BORGSTROM F., KANIS J.A., COMPSTON J., COOPER C., MCCLOSKEY E.V., JOHSSON B., *Osteoporosis: burden, health care provision and opportunities in the EU*, Arch. Osteoporos., 2011, 6, 59–155.
- [24] STURMER E.K., SEIDLOVA-WUTTKE D., SEHMISCH S., RACK T., WILLE J., FROSCHE K.H., WUTTKE W., STURMER K.M., *Standardized Bending and Breaking Test for the Normal and Osteoporotic Metaphyseal Tibias of the Rat: Effect of Estradiol, Testosterone, and Raloxifene*, J. Bone Min. Res., 2006, 21, 89–96.
- [25] UDHAYAKUMAR G., SUJATHA C.M., RAMAKRISHNAN S., *Comparison of two interpolation methods for empirical mode decomposition based evaluation of radiographic femur bone images*, Acta Bioeng. Biomech., 2013, 15, 73–80.
- [26] VERHULP E., RIETBERGEN B., HUISKES R., *Load distribution in the healthy and osteoporotic human proximal femur during a fall to the side*, Bone, 2008, 42, 30–35.
- [27] ZHANG L., LU H., ZHENG H., LI M., YIN P., PENG Y., GAO Y., ZHANG L., TANG P., *Correlation between Parameters of Calcaneal Quantitative Ultrasound and Hip Structural Analysis in Osteoporotic Fracture Patients*, PLoS ONE, 2015, 10, 1–14.
- [28] ZHOU Y., MIN L., LIU Y., SHI R., ZHANG W., ZHANG H., DUAN H., TU CH., *Finite element analysis of the pelvis after modular hemipelvic endoprosthesis reconstruction*, Int. Orthop., 2013, 37, 653–658.